

Date of publication xxxx 00, 0000, date of current version xxxx 00, 0000.

Digital Object Identifier 10.1109/ACCESS.2017.Doi Number

# Brain Tumor Identification and Classification of MRI images using deep learning techniques

Zhesu Jia, Deyun Chen\*

School of Computer Science and Technology, Harbin University of Science and Technology, Harbin 150080, China

chen\_deyun@126.com

## Abstract

The detection, segmentation, and extraction from Magnetic Resonance Imaging (MRI) images of contaminated tumor areas are significant concerns; however, a repetitive and extensive task executed by radiologists or clinical experts relies on their expertise. Image processing concepts can imagine the various anatomical structure of the human organ. Detection of human brain abnormal structures by basic imaging techniques is challenging. In this paper, a Fully Automatic Heterogeneous Segmentation using Support Vector Machine (FAHS-SVM) has been proposed for brain tumor segmentation based on deep learning techniques. The present work proposes the separation of the whole cerebral venous system into MRI imaging with the addition of a new, fully automatic algorithm based on structural, morphological, and relaxometry details. The segmenting function is distinguished by a high level of uniformity between anatomy and the neighboring brain tissue. ELM is a type of learning algorithm consisting of one or more layers of hidden nodes. Such networks are used in various areas, including regression and classification. In brain MRI images, the probabilistic neural network classification system has been utilized for training and checking the accuracy of tumor detection in images. The numerical results show almost 98.51% accuracy in detecting abnormal and normal tissue from brain Magnetic Resonance images that demonstrate the efficiency of the system suggested.

**Keywords:** Brain Tumor Detection, Classification, Segmentation, Deep learning, ELM

## 1. The Importance and Significance of Detecting Brain Tumors

In clinical studies on brain anatomy, MRI has become a crucial tool [1]. The high resolution, contrast, and clear separation of the soft tissue enable doctors to identify specific diseases accurately [2]. For understanding pathology, for assessing evolutionary trends, for preparation, the best surgical method or alternatives possible, an exact segmentation of the pathological and healthy tissues that comprise the Magnetic Resonance image are necessary [3]. Automated segmentation methods are a helpful solution to help management with unreliable degrees of automation to trace the boundaries of various tissue areas, and by allowing automated volumetric of pathologic MRI signal analysis [4]. The tumor represents uncontrolled cancer cell growth in any part of the body, while a tumor in the brain is an abandoned brain cell growth Benign or malignant may be a brain tumor [5]. The benign brain tumor is structurally similar and does not include active (cancer) cells, while malignant (heterogeneous) tumors contain active (cell) cells [6]. Meningioma and Gliomas are low-grade cancer known as benign tumors and high-grade tumors classified as malignant tumors, including astrocytoma and glioblastoma [7]. Glioblastoma is the most malignant type of astrocytoma, the most elevated glioma [8]. Glioblastoma is unique to all other forms of the tumor class from the abnormally rapid growth of

blood vessels and the development of necrosis (dead cells) more or less the tumor [9].

In cancer treatment plans and cancer research, it is essential to segment the pathological and healthy brain tissues from MRI with their sub-regions [10]. The segmentation of images remains a crucial task for all medical image processing techniques, which consists of eliminating regions of interest from images [11]. [12] This operation is too long, tedious, and in some cases, challenging, given the immense amounts of data that every image provides [13]. In general, when segmenting brain tumor images, the radiologist considers all these MRI approaches concurrently [14]. Standard brain tumor clinical acquisition protocols provide a high-resolution intra-slice, low inter-slice space [15]. It creates a further obstacle for automated analysis [16]. To overcome all these challenges, a new methodology that has been developed and it's clinically focused and takes advantage not only of advanced imaging technologies takes into account the type of information that is typically available for patient and large-scale clinical therapy plans [17]. Figure 1 (a) shows the 2D model of brain tumor detection, and 1(b) shows the MRI image of a brain tumor

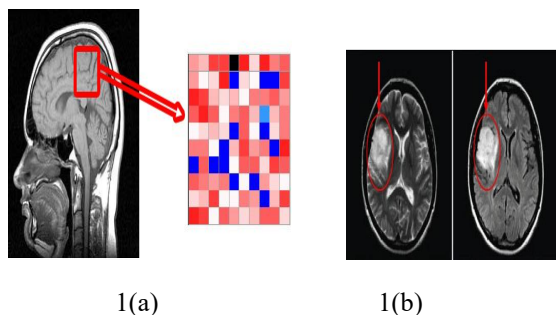


Figure 1: (a) 2D Model of Brain Tumor Detection (b) MRI image of a brain tumor [18]

This work focuses on the automated segmentation of meningioma from MR imaging in multi-spectral brain datasets. One of the few benign tumors determined in the brain region is a meningioma [19]. Accurate tumor identification leads to the development of surgical indications in elderly persons who are carrying intracranial meningioma [20]. In recent years, Support Vector Machine (SVM) methods in MRI segmentation aimed at determining a range of neurological conditions have demonstrated excellent performance [21]. Segmentation is used for the identification of contaminated tumor tissues from modes of medical imaging [22]. In image analysis, segmentation is necessary and essential; it is a procedure of dividing an image into various blocks or regions which share common and identical characteristics like gray level, texture, color, contrast, boundaries, and brightness [23].

The significant contribution of this paper is:

- To propose Fully Automated Heterogeneous Segmentation using Support Vector Machine (FAHS-SVM) for brain tumor detection and segmentation.
- To design an Extreme learning machine algorithm for the classification and feature extraction of MRI images.
- The experimental results show high accuracy in detecting brain tumors with the help of datasets.

The remainder of the paper discussed as follows: Section 1 and Section 2 discussed the importance of detecting brain tumor and background review. In section 3, a Fully Automated Heterogeneous Segmentation using Support Vector Machine (FAHS-SVM) has been proposed for brain tumor segmentation based on deep learning techniques. In section 4, the experimental results have been demonstrated. Finally, section 5 concludes the research article.

## 2. Background Review and Features of this Research Paper

P.Mohamed Shakeel et al. [24] proposed the machine learning-based Back propagation neural network (MLBPNN) method for brain tumor classification systems. Besides, the system can help doctors utilizing order and package calculations to scan the picture cell by coloring telephone qualities. The various steps needed in the preparation of the images from biopsy pictures to locate a disease include acquisition, upgrading and division,

extraction, picture representation, characterization, and essential management. MLBPNN is analyzed using infrared sensor imaging technology in this study. Instead, when the entire structure is degraded in some subsystems, the multidimensional machine existence of distinguishing neural proof unbelievably decreases. This image sensor is integrated via a Wireless Infrared Imaging Sensor that transfers the warm tumor data to a medical specialist to screen the well-being situation and to usefully control the level of ultrasound measurement, especially if elderly patients in remote areas are present.

Ali ARI et al. [25] introduced the Extreme learning machine local receptive fields (ELM-LRF) for brain tumor classification and detection. First of all, non-local means and methods of local smoothing have been utilized to neglect noises. In the second step, the use of ELM-LRF identified cranial magnetic resonance (MR) images as malignant or benign. The tumors were segmented in the third phase. The purpose of this study was only to use cranial MR images that have mass. The classification exactness of cranial MR images is 96.2 % in the experimental studies. The findings analyzed showed that the efficiency of the suggested approach was higher than that of other recent literature studies. Experimental results have shown that it is an effective method that can be used to diagnose computer-aided brain tumors.

Nilesh Bhaskarrao Bahadur et al. [26] initialized the Berkeley Wavelet Transformation and Support Vector Machine (BWT-SVM) for image analysis for Magnetic Resonance images based Brain Tumor identification and feature extraction. They explored histogram-based and texture-based features with an approved MR brain tumor classification classifier. The tests for brain tumor diagnosis can be seen quickly and accurately from the experimental results in the various images in contrast with manual identification by clinical experts or radiologists. The different performance variables show a better result with the proposed algorithm by enhancing other parameters such as PSNR, mean, MSE, precision, specificity, sensitivity, coefficient of dice.

Jason J. Corso et al. [27] introduced the Multilevel Segmentation by Weighted Aggregation (MSWA) for brain tumor segmentation. A new way of automatically segmenting heterogeneous imaging data is to bridge the gap between affinity-based, bottom-up, and top-down model-based methods. The paper's significant contribution is a Bayesian algorithm for integrating soft model tasks in the measurement of affinities that are usually free of models. The effective computational approach exceeds current techniques in order of magnitude that offers comparable or enhanced results. Their quantitative outcomes show that model affinities are integrated into the segmentation procedures for the hard case of brain tumors. This approach blends the essential section of each voxel with the essential part of the graph hierarchy. The system is independent of each voxel, and the neighborhood data is integrated implicitly because the graphical hierarchy is agglomerated.

Pradeep Kumar Mallick et al. [28] suggested the Deep wavelet Auto Encoder and Deep Neural Network (DWA-DNN) for Brain Magnetic Resonance image classification for cancer recognition. This paper proposes a Deep Wavelet Auto Encoder (DWA) image compression technique, which combines the Auto Encoder essential feature extraction function with the transform wavelet image decomposition method. The mixture of both has a tremendous impact on the reduction of the feature set to continue to identify with DNN. The suggested DWA-DNN image classifier was reviewed, and a brain picture dataset was taken. In comparison to other classifiers like Auto Encoder - DNN or DNN, the efficient criterion for the DWA-DNN was compared, and the approach suggested summarizes the methods that exist. The tests of the DWA-DNN approach proposed to show that it is much more accurate and predictive than any other deep learning methodology. Further finding a way to combine DNN with many other improvements in the Auto Encoder would be far more interesting to see the impact or results within the brain MRI dataset [29-33].

To overcome these issues, in this paper, a Fully Automatic Heterogeneous Segmentation using Support Vector Machine (FAHS-SVM) has been proposed for brain tumor segmentation based on deep learning techniques. A supervised method for the

segmentation of the brain image, which is the Support Vector Machines (SVM) classification process, has been utilized. To use the support vector machine (SVM) can identify brain tumors in many MRI modalities. The proposed system reviews segmentation as a classification issue. More accurately, because it is crucially faster than other classification techniques, because of its robustness in generalization precipitation and its capacity to manage volume information, the SVM classification method ensures segmentation.

### 3. A Fully Automatic Heterogeneous Segmentation using Support Vector Machine (FAHS-SVM):

In this study, a Fully Automatic Heterogeneous Segmentation using Support vector machine (FAHS-SVM) for brain tumor detection and segmentation. Figure 2 describes the proposed FAHS-SVM method architecture. Magnetic Resonance Imaging is a diagnostic tool for human anatomy study and testing. Increased tumor vascularity leads to preferential uptake of the contrasting agent and can be utilized better to view the tumors of the normal tissue around them. When the contrast injections are performed repeatedly, the dynamic nature of contrast uptake can be tested, which can increase the distinction between malignant or benign diseases.

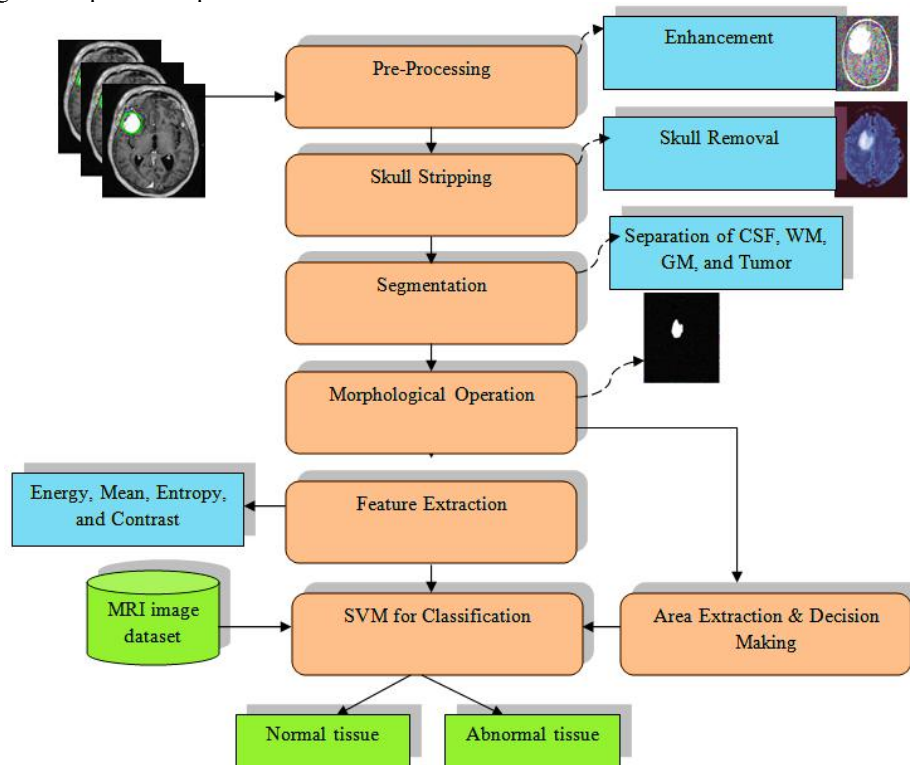


Figure 2: The proposed FAHS-SVM method architecture

#### i) Pre-Processing:

The primary operation of pre-processing is to enhance the quality of the Magnetic Resonance images and to make them suitable for further processing via a human visual for people or computers. Pre-processing leads to improving specific Magnetic

Resonance image parameters like the enhanced SNR ratio, the improvement of the visual look of the Magnetic Resonance Image, the elimination of unnecessary noise, and the underseen parts from the picture, smoothing the region's inner part and retaining its edges. To apply adaptive contrast improvement

based on a changed sigmoid feature to enhance the SNR ratio and, therefore, the quality of the raw Magnetic Resonance images.

## ii) Skull Stripping:

Skull stripping is a major biomedical image analysis procedure. It is essential for a practical test of brain tumors from MR images, in which all non-brain tissue in brain imaging is removed. Skull stripping enables additional brain tissues like skull, skin, and fat to be extracted in brain images. There are a variety of skull stripping techniques available, some of which are common include the use of an automated skull stripping by image contour, segmentation-and morphological stripping of the skull, and hectographic analysis or threshold-based skull stripping.

## iii) Morphological Operation and Segmentation:

In the first stage, the pre-processed brain Magnetic Resonance image will be transformed into a binary image with a threshold of 128 for the cutoff. Pixel values higher than the specified thresholds are mapped as white, with other regions marked as black; these two allow various regions to be generated around the disease. In the second stage, an erosion process of morphology is used to extract white pixels. Eventually, the eroded area and the original image are separated into two equal areas, and the region with black pixels from the eroding is counted as a mask of brain Magnetic Resonance image. In this paper, wavelet transformation is used for the efficient segmentation of the brain Magnetic Resonance image. Figure 3 shows the fully automatic heterogeneous segmentation. Figure 3(a) shows the axial image and its segmentation figure 3(b) Coronal image and its segmentation figure 3 (c) Sagittal images and its segmentation.

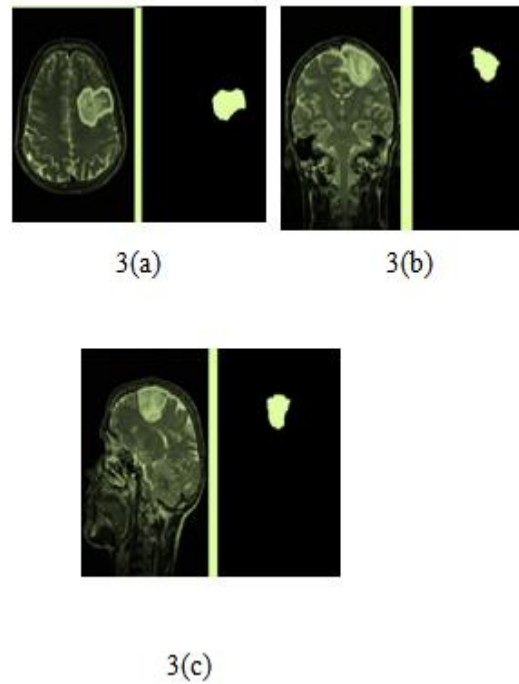


Figure 3: Fully Automatic Heterogeneous segmentation (a) Axial image and its segmentation (b) Coronal image and its segmentation (c) Sagittal image and its segmentation

A wavelet is a function stated over a limited time interval with an average value of null. The transformation wavelet method is used to create features, operators, and data into different frequency components, which allows every component to be discretely studied. All wavelets are produced from a basic wavelet  $\varphi(r)$  utilizing the translation and scaling procedure stated by equation (1); A simple wavelet is called a mother wavelet due to the other wavelets it is the point of origin.

$$\varphi_{w,\tau} = \frac{1}{\sqrt{w}} \varphi\left(\frac{r-\tau}{w}\right) \quad (1)$$

As shown in equation (1), where  $w$  and  $\tau$  are the translation and scale factors correspondingly.

The efficient way of the depiction of image transformation and  $\alpha_\theta^\varphi$  is a piecewise constant function and it generates a different pixel position in the 2D plane via translation and scaling of wavelet and expressed as,

$$\alpha_\theta^\varphi(\tau,w) = \frac{1}{w^2} \alpha_y^\varphi(3^w(y-j), 3^w(x-i)), \quad (2)$$

As shown in equation (2), where  $\tau$  and  $w$  are translation and scale variable of the wavelet transformation. The only constant term sufficiently depicts an image mean value; in the single term, the coefficient value is shown

$$\alpha_0 = \frac{1}{\sqrt{9}} \left[ v \left( \frac{y}{3}, \frac{x}{3} \right) \right] \quad (3)$$

The morphological procedure is used for extracting the limits of the brain images. Conceptually, only the relative order of the pixel values is restructured in morphological operation, not their mathematical values, and only binary images can, therefore, be processed. Dilatation operations are intended to insert pixels into an object's boundary area and to delete pixels from the object boundary zone. Addition and pixel removal operations depend on the structuring aspect of the selected picture from or to the boundary region of objects. The results of the experiment provided by the proposed procedure are shown for the segmented results of the CSF, GM, and WM, classes, and the tumor region extracted.

#### iv) Feature Extraction:

It is the set of superior-level image details, including contrast, shape, color, and texture. In reality, texture analysis is a crucial attribute for the vision and machine learning systems of humans. It is utilized efficiently by choosing prominent features to maximize the precision of the diagnostic system. Due to the complex structure of different tissues like CSF, WM, and GM in the brain images MR, it's a crucial challenge to obtain relevant features. The diagnosis of the tumor (tumor stage) could be enhanced by textual observations and analyses, as well as the therapy response assessment. Some of the useful features can be found below in the mathematical formula.

**A. Mean:** The mean of an image is determined by summing up an image total pixel values divided by the total pixel value of an image.

$$N = \left(\frac{1}{n \times m}\right) \sum_{y=0}^{n-1} \sum_{x=0}^{m-1} f(y,x) \quad (4)$$

**B. Standard Deviation:** The SD is the second central moment in which an observed population can be described as the probability distribution and to calculate of inhomogeneity. A better value shows a good level of intensity and great contrast between the edges of an image.

$$SD(\rho) = \sqrt{\left(\frac{1}{n \times m}\right) \sum_{y=0}^{n-1} \sum_{x=0}^{m-1} (f(y,x) - N)^2} \quad (5)$$

**C. Entropy:** Entropy is measured to characterize the textured image randomness and is defined as

$$D = - \sum_{y=0}^{n-1} \sum_{x=0}^{m-1} f(y,x) \log_2 f(y,x) \quad (6)$$

**D. Skewness:** Skewness is a symmetry attribute or symmetry absence. The Skewness is called  $W_l(Y)$  and defined as a random variable Y.

$$W_l(Y) = \left(\frac{1}{n \times m}\right) \frac{\sum (f(y,x) - N)^3}{SD^3} \quad (7)$$

**E. Kurtosis:** The parameter Kurtosis defines the shape of a random variable likelihood distribution. The Kurtosis is referred to as  $L(Y)$  for random variable Y and is defined as

$$L(Y) = \left(\frac{1}{n \times m}\right) \frac{\sum (f(y,x) - N)^4}{SD^4}$$

**F. Energy:** Energy can be stated as the amount of pixel-pair reproductions that can be quantified. Energy is a parameter for calculating an image's similarity. If the Haralick's GLCM function defines energy, it is known as an angular second moment and is stated as

$$Em = \sqrt{\sum_{y=0}^{n-1} \sum_{x=0}^{m-1} f^2(y,x)} \quad (9)$$

**G. Contrast:** Contrast is a calculation of the intensity and the neighbor of a pixel over the image.

$$G = \sum_{y=0}^{n-1} \sum_{x=0}^{m-1} (y - x)^2 f(y,x) \quad (10)$$

**H. Homogeneity or Inverted moment of difference (IDM):** The IDM is a calculation of an image's local consistency IDM could have a single value or set of benefits to identify whether or not the model is textured.

$$IDM = \sum_{y=0}^{n-1} \sum_{x=0}^{m-1} \frac{1}{1+(y-x)^2} f(y,x) \quad (11)$$

**I. Direction moment:** Direction moment is a textural feature of the image measured by taking into account the angle of alignment of the image, and it is defined as

$$DM = \sum_{y=0}^{n-1} \sum_{x=0}^{m-1} f(y,x) |y - x| \quad (12)$$

**J. Correlation:** The correlation feature explains and determines the spatial dependencies between the pixels,

$$C = \frac{\sum_{y=0}^{n-1} \sum_{x=0}^{m-1} (y,x) f(y,x) - N_y N_x}{\rho_y \rho_x} \quad (13)$$

As shown in equation (12) where  $\rho_y$  and  $N_y$  and are the standard deviation and mean in the horizontal spatial domain and  $\rho_x$  and  $N_x$  are standard deviation and mean in the vertical spatial domain.

**K. Coarseness:** Coarseness is the textural analysis of an image is the measure of roughness. For a fixed window size, the texture is said to be coarser than the one with a higher number with a smaller number of texture attributes. The rougher layer is coarser. Smaller coarseness values have fine textures. The meaning is:

$$H = \frac{1}{2^{n+m}} \sum_{y=0}^{n-1} \sum_{x=0}^{m-1} f(y,x) \quad (14)$$

In addition to the above-mentioned textural feature extraction, the following criteria of quality evaluation are required to improve the results of MR images in the brain.

**L. The Structural Similarity Index (SSIM):** SSIM is a perceptual metric indicating the probability that data compression or loss in data transmission or by any other means

of image processing will result in quality degradation. The meaning is that

$$SSIM = \left( \frac{\rho_{yx}}{\rho_y \rho_x} \right) \left( \frac{2\bar{y}\bar{x}}{(\bar{y}^2 + \bar{x}^2) + B_1} \right) \left( \frac{2\rho_y \rho_x}{(\rho_y^2 + \rho_x^2) + B_2} \right) \quad (15)$$

A higher SSIM value means that luminance, contrast, and structural quality are maintained very efficiently.

**M. Mean square error:** MSE is fidelity image or signal fidelity. To find a correlation or truth between two models, the signal or image fidelity calculation seeks to provide a quantitative score. When Mean Square Error is measured, one image is presumed to be impure, the other to be distorted or manipulated by some means and described as "original."

$$MSE = \frac{1}{N \times M} \sum \sum (f(y,x) - f^T(y,x))^2 \quad (16)$$

**N. Peak Signal to Noise Ratio:** The PSNR is a calculation used for the evaluation of the accuracy of the image reconstruction.

$$PSBR \text{ in db} = 20 \log_{10} \frac{2^m - 1}{MSE} \quad (17)$$

An excellent signal-to-noise ratio suggests lower MSE values and a higher PSNR value.

**Algorithm 1: Extreme learning machine algorithm based on SVM**

```

Input: j,I
Output: l, x
For (i=0)
f(x) = ZRω(x) + a
For (j=0)
l(xj,xi) = exp [ - δ ||xj - xi||2 ]
If (I=0)
l(xj,xi) = ∑j=1M ∑Yi ∈ Ni ( exp [ - δ ||xj - xi||2 ] )
Else (I>0)
l(xj,xi) = ∑j=1M ∑Yi ∈ Ni ( exp [ - δ ||xj - xi||2 ] ) = 1
End if
End for
End for
End
Return
    
```

As shown in algorithm 1, the extreme learning machine algorithm based on the SVM classifier. ELM's essence consists of randomly assigning the learning parameters of hidden nodes involving biases and input weights and not requiring configuration while analytically evaluating output weights by the simple generalized inverse operation. ELM, in many cases, tends to need hidden neurons rather than standard tuning algorithms. Since the biases and weights of the hidden layer are altered, and the weighing of the outputs are analytically

calculated by purely numerical manipulation, extreme learning machine has low calculation time for training for new classifiers.

The SVM algorithm is the basis of the analysis of a supervised learning method, applied to a classification issue in them-class. The primary purpose of the SVM algorithm is to turn a nonlinear divisive goal into a linear transformation utilizing a feature called the SVM kernel function. The transformation function has been used in the Gaussian kernel. The use of a kernel function allows nonlinear samples to be converted into a high-dimensional future space where samples data or nonlinear samples can be isolated or graded. A hyperplane divided into two training is known as the SVM algorithm,

$$f(x) = Z^R \omega(x) + a \quad (18)$$

As shown in equation (18) where Z and R, hyperplane parameter and ω(x) is a function utilized to map vector x into a more significant dimensional space. The equation (19) gives the nonlinear SVM Gaussian Kernel function used for the Generalization and classification optimal solution and its advanced classification features in equation (20),

$$l(x_j, x_i) = \exp \left[ - \delta \|x_j - x_i\|^2 \right] \quad (19)$$

$$l(x_j, x_i) = \sum_{j=1}^M \sum_{Y_i \in N_i} \left( \exp \left[ - \delta \|x_j - x_i\|^2 \right] \right) \quad (20)$$

As shown in the above equation where x<sub>j</sub> and x<sub>i</sub> are objects j and I correspondingly, and δ is a contour attribute utilized to identify the boundary field smoothness.

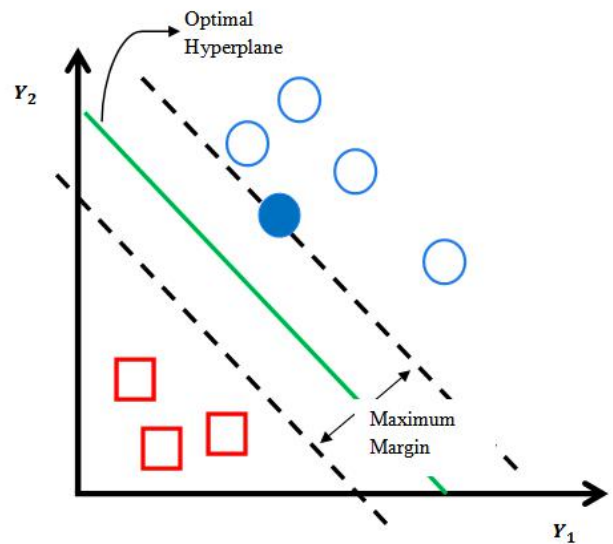


Figure 4: Graphical Representation of SVM based on linearly separable data

The kernel-class selection features make SVM the default choice for brain tumor classification. The efficiency of the SVM algorithms can be measured by the accuracy, sensitivity, and specificity of the words TN, TP, FN, and FP the result of

accuracy ground truth, specificity, and sensitivity. Figure 4 shows the Graphical Representation of SVM based on linearly separable data. Section 4 illustrates the experimental results of the proposed FAHS-SVM method.

#### 4. Experimental Result Analysis

##### (i) Dice Similarity Coefficient

The Dice similarity coefficient is utilized to assess the results quantitatively. In a manual segmentation, the ground truth has been established. The manual segmentation of the tumor tissues has not available for healthy tissues, however. Therefore, it can be assessed quantitatively only the exactness of the tumor

segmentation. Only visual inspection has necessary to determine the accuracy of the segmentation of healthy tissues qualitatively. Dice similarity coefficient is an overlap measure between two images and defined as,

$$Dice(B, A) = 2 \times \frac{|B_1 \cap A_1|}{(|B_1| + |A_1|)} \quad (21)$$

As shown in equation (21) where  $A \in \{0,1\}$  is the expert's ground truth and  $B \in \{0,1\}$  is a tumor region extracted from algorithmic predictions. The dice coefficient, the maximum value 1, and the minimum value are 0, while the higher value means a good overlap between the two images. Figure 5 shows the Dice similarity coefficient for the proposed FAHS-SVM method.

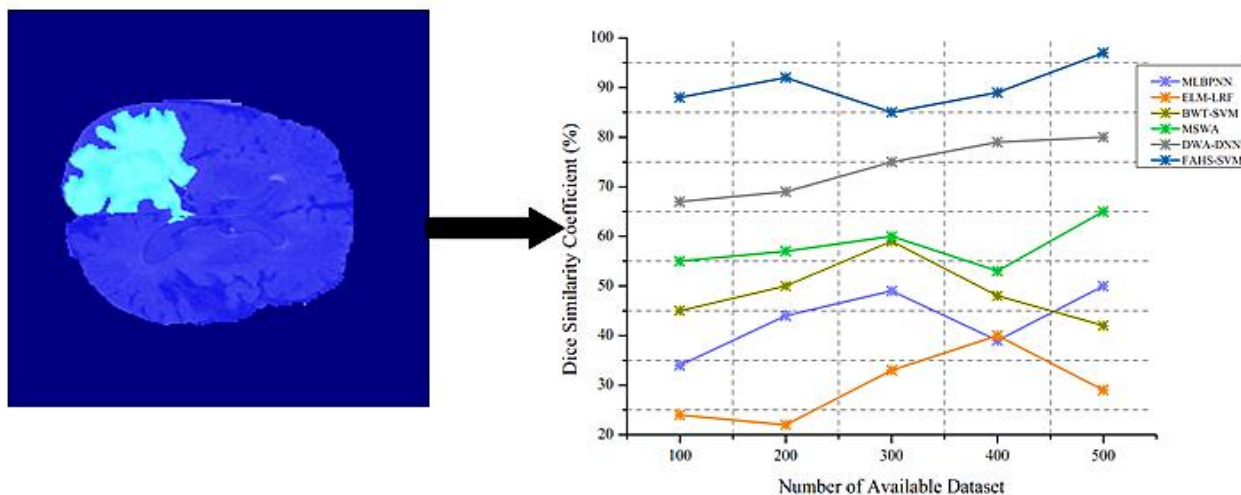


Figure 5: Dice Similarity Coefficient

Table 1 demonstrates the dice similarity coefficient of the proposed FAHS-SVM method (Mean and Standard Deviation). The gross tumor region, including active, necrotic, and edema parts, comprises a gross tumor volume (GTV). The findings are provided with and without regularization for intra-and inter-patient (leave-one-out cross-validation). The dice coefficients for each sub-region of the tumor are lower. The results, however, show once again that if no hierarchical regulation is applied, the Dice coefficient is worse.

Table 1: Dice Similarity Coefficient

Number of Available Datasets	MLBPNN	ELM-LRF	BWT-SVM	MSWA	DWA-DNN	FAHS-SVM
100	34.5	24.4	45.6	55.7	66.1	89.3
200	42.1	21.6	50.9	56.3	74.4	92.4
300	48.2	32.5	56.4	57.3	75.8	85.6
400	39.6	40.4	48.7	54.2	83.4	91.2

500	50.4	29.8	43.6	65.1	85.6	97.6
-----	------	------	------	------	------	------

##### (ii) Segmentation Accuracy Analysis

The accuracy of our automated system is similar to the values recorded for manual segmental inter-observer variability. Finally, a robust initialization of labeling is created, taking both SVM and high-profile candidate regions into account. Results of the validation experiment on multi-parametric images showed that increased accuracy in tumor segmentation relative to state-of-the-art methods could be achieved. Tissues with brain structures are complex, and their intensity features are not sufficient to precisely segment the tumor. To improve the accuracy of segmentation, texture features are used. The textural features are evaluated based on texture analysis in this review. Textons are small image elements generated by an image convolution with a particular filter bank. The accuracy of segmentation is high when compared to other existing methods. Figure 6 demonstrates the segmentation accuracy analysis of the suggested FAHS-SVM approaches.

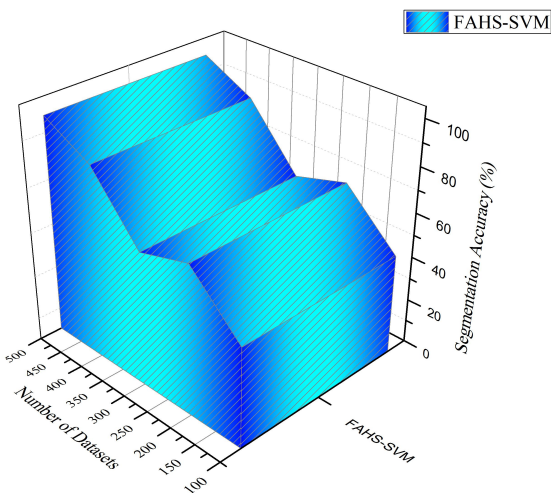


Figure 6: Segmentation Accuracy Analysis

**(iii)Fractal Dimension vs. Mean Intensity**

From the binary channels, which involve area intensity and fractal dimension, the fractal features are measured. The feature area is the super-pixel number of edge pixels. The intensity of pixels respective to edge pixels in a super-pixel is the mean intensity of the images. The fractal dimension depicts the difficulty of the image structure and is measured as:

$$C_0 = \lim_{\epsilon \rightarrow 0} \frac{\log M(\epsilon)}{\log \epsilon^{-1}} \quad (22)$$

As shown in equation (22), where  $M(\epsilon)$  indicates the counting of hypercubes of dimensions  $E$  and length  $\epsilon$ . It shows a good separation for MRI images in the feature space (mean intensity fractal dimension). Figure 7 demonstrates the fractal dimension vs. the mean intensity of the proposed FAHS-SVM method.

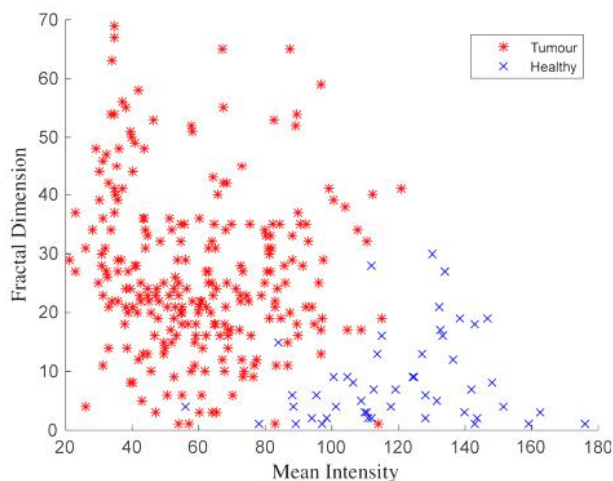


Figure 7: Fractal Dimension vs. Mean Intensity

**(iv)Probability of Detection Ratio**

A broad range of features such as intensity textures, label lengths, spatial tissue prior probabilities, and current work can be measured for each image and combine many of them based on the nature of the issue. Based on training images for the complex classification outcome and the classification probabilities for images of the tumor, tumor-sampling map and non-tumor-sample map, an SVM two-class classification to differentiate tumor from normal tissues are created. The tumor sample map shows voxel-level tumor salience. The proposed FAHS-SVM method has a high probability of detecting brain tumors when compared to other MLBPNN, ELM-LRF, BWT-SVM, MSWA, and DWA-DNN methods. Figure 8 demonstrates the probability of the detection ratio of the proposed FAHS-SVM method.

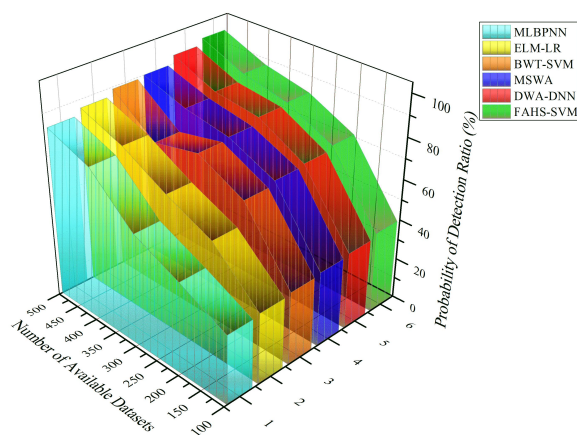


Figure 8: Probability of Detection Ratio

Table 2 demonstrates the probability of detection ratio evaluation of the suggested FAHS-SVM method. The probabilistic neural network classifier has been employed to train and test for tumor accuracy in brain MRI images. Brain tumor detection at a very early stage has a crucial issue so that proper therapy could be taken. Much effective segmentation could not be performed with combined feature extraction, and few features have been extracted, which led to low tumor identification and detection accuracies.

Table 2: Probability of Detection Ratio Evaluation

Number of Available Datasets	MLBPNN	ELM-LRF	BWT-SVM	MSWA	DWA-DNN	FAHS-SVM
100	33.2	35.4	37.4	38.9	40.1	41.3
200	44.2	45.6	56.7	59.8	60.2	63.1
300	55.3	59.8	67.8	69.5	73.2	74.2
400	76.3	78.9	80.2	84.9	86.8	87.5
500	83.2	88.3	90.2	95.6	96.7	98.8



## (v) Classification Error

Tumor size affects the accuracy of segmentation, and tumor boundaries are usual errors. Large brain tumors are defined by a high number of misclassified image pixels. Furthermore, large tumors probably enter the brain and CSF and make it challenging to determine the boundary of the tumor accurately. The proposed system controlled volume MRIs with different features, including many slices and tumor size, form, border, and position concerning the overall executive processing time. The overall segmentation process takes time because of these characteristics. Therefore, the processing time of the system proposed has been lastly measured. The proposed method has less classification error when compared to other existing methods. Figure 9 shows the classification error of the proposed FAHS-SVM method.

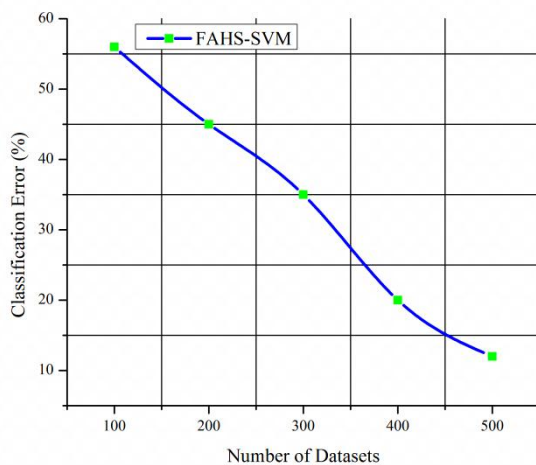


Figure 9: Classification Error

The extraction phase features calculate an intensity and system characterized vector for each pixel. Subsequently, SVM develops a classification model providing the distinction between pixels of tumors and normal. Finally, the new pixels are classified to extract tumor areas (i.e., the set of tumor pixels). The method FAHS-SVM in brain tumor segmentation is useful because the technique takes into account not only local tumor properties such as gradients and global aspects such as the size of the tumor, shape length and region length. Although the accuracy achieved and has been high relative to other segmentation techniques, for the segmentation of brain tumors, the FAHS-SVM has relatively slow. A considerable number of MRI slices pixel resolution has been processed at such a slow pace with a high number of iterations to achieve the required accuracy.

## 5. Conclusion

This paper presents a Fully Automatic Heterogeneous Segmentation using Support Vector Machine (FAHS-SVM) for brain tumor identification and segmentation. The accuracy of

our automated approach is similar to the values for manual segmentation inter-observer variability. To identify tumor regions by combining intrinsic image structure hierarchy and statistical classification information. The tumor areas described are spatially small and consistent concerning image content and provide an appropriate and robust guide for the consequent segmentation. The proposed method can achieve promising tumor segmentation in conjunction with a semi-supervised approach under a local and globalized accuracy system, as is shown by experiments focused on multi-parametric Magnetic Resonance images. Our experimental results indicate that the method proposed will help to identify the exact location of the brain tumor accurately and quickly. The proposed method is, therefore, critical for MR imagery brain tumor detection. The experimental results showed 98.51% of the accuracy of the proposed technology in the detection of abnormal and normal tissues in Magnetic Resonance images. The findings lead to the end that the suggested approach is sufficient for the inclusion of primary diagnostic and radiologist or clinical experts in support of clinical decision systems.

## Acknowledgment

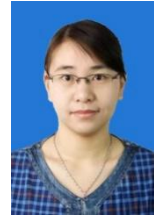
This paper is funded by the National Natural Science Foundation of China (No. 60572153; No. 60972127).

## Reference

1. Mohsen, H., El-Dahshan, E. S. A., El-Horbaty, E. S. M., & Salem, A. B. M. (2018). Classification using deep learning neural networks for brain tumors. *Future Computing and Informatics Journal*, 3(1), 68-71.
2. Işın, A., Direkçoğlu, C., & Şah, M. (2016). Review of MRI-based brain tumor image segmentation using deep learning methods. *Procedia Computer Science*, 102, 317-324.
3. Rathi, V. G. P., & Palani, S. (2015). Brain tumor detection and classification using deep learning classifiers on MRI images. *Research Journal of Applied Sciences, Engineering, and Technology*, 10(2), 177-187.
4. Sobhaninia, Z., Rezaei, S., Noroozi, A., Ahmadi, M., Zarrabi, H., Karimi, N., ... & Samavi, S. (2018). Brain tumor segmentation using deep learning by type-specific sorting of images. *arXiv preprint arXiv:1809.07786*.
5. Pan, Y., Huang, W., Lin, Z., Zhu, W., Zhou, J., Wong, J., & Ding, Z. (2015, August). Brain tumor grading based on neural networks and convolutional neural networks. In *2015 37th Annual International Conference of the IEEE Engineering in Medicine and Biology Society (EMBC)* (pp. 699-702). IEEE.
6. Hussain, S., Anwar, S. M., & Majid, M. (2018). Segmentation of glioma tumors in the brain using deep convolutional neural network. *Neurocomputing*, 282, 248-261.
7. Dong, H., Yang, G., Liu, F., Mao, Y., & Guo, Y. (2017, July). Automatic brain tumor detection and segmentation using unit-based fully convolutional networks. *An annual conference on medical image understanding and analysis* (pp. 506-517). Springer, Cham.
8. Sajjad, M., Khan, S., Muhammad, K., Wu, W., Ullah, A., & Baik, S. W. (2019). Multi-grade brain tumor classification using deep CNN with extensive data augmentation. *Journal of computational science*, 30, 174-182.
9. Korfiatis, P., Kline, T. L., & Erickson, B. J. (2016). Automated segmentation of hyperintense regions in FLAIR MRI using deep learning. *Tomography*, 2(4), 334.
10. Hussain, S., Anwar, S. M., & Majid, M. (2017, July). Brain tumor segmentation using cascaded deep convolutional neural network.

In *2017 39th Annual International Conference of the IEEE Engineering in Medicine and Biology Society (EMBC)* (pp. 1998-2001). IEEE.

11. Zhao, X., Wu, Y., Song, G., Li, Z., Zhang, Y., & Fan, Y. (2018). A deep learning model integrating FCNNs and CRFs for brain tumor segmentation. *Medical image analysis*, 43, 98-111.
12. Deepak, S., & Ameer, P. M. (2019). Brain tumor classification using deep CNN features via transfer learning. *Computers in biology and medicine*, 111, 103345.
13. Amin, J., Sharif, M., Yasmin, M., & Fernandes, S. L. (2018). Big data analysis for brain tumor detection: Deep convolutional neural networks. *Future Generation Computer Systems*, 87, 290-297.
14. Sajid, S., Hussain, S., & Sarwar, A. (2019). Brain tumor detection and segmentation in MR images using deep learning. *Arabian Journal for Science and Engineering*, 44(11), 9249-9261.
15. Nie, D., Zhang, H., Adeli, E., Liu, L., & Shen, D. (2016, October). 3D deep learning for multi-modal imaging-guided survival time prediction of brain tumor patients. In *International conference on medical image computing and computer-assisted intervention* (pp. 212-220). Springer, Cham.
16. Xu, Y., Jia, Z., Ai, Y., Zhang, F., Lai, M., Eric, I., & Chang, C. (2015, April). Deep convolutional activation features for large scale brain tumor histopathology image classification and segmentation. In the *2015 IEEE international conference on acoustics, speech and signal processing (ICASSP)* (pp. 947-951). IEEE.
17. Pereira, S., Pinto, A., Alves, V., & Silva, C. A. (2016). Brain tumor segmentation using convolutional neural networks in MRI images. *IEEE transactions on medical imaging*, 35(5), 1240-1251.
18. <http://pubs.sciepub.com/jbet/1/3/3/index.html>
19. Xiao, Z., Huang, R., Ding, Y., Lan, T., Dong, R., Qin, Z., ... & Wang, W. (2016, October). A deep learning-based segmentation method for a brain tumor in MR images. In *2016 IEEE 6th International Conference on Computational Advances in Bio and Medical Sciences (ICCBMS)* (pp. 1-6). IEEE.
20. Saba, T., Mohamed, A. S., El-Affendi, M., Amin, J., & Sharif, M. (2020). Brain tumor detection using the fusion of handcrafted and deep learning features. *Cognitive Systems Research*, 59, 221-230.
21. Chato, L., & Latifi, S. (2017, October). Machine learning and deep learning techniques to predict the overall survival of brain tumor patients using MRI images. In *2017 IEEE 17th International Conference on Bioinformatics and Bioengineering (BIBE)* (pp. 9-14). IEEE.
22. Have, M., Davy, A., Warde-Farley, D., Biard, A., Courville, A., Bengio, Y., ... & Larochelle, H. (2017). Brain tumor segmentation with deep neural networks. *Medical image analysis*, 35, 18-31.
23. Mittal, M., Goyal, L. M., Kaur, S., Kaur, I., Verma, A., & Hemant, D. J. (2019). Deep learning-based enhanced tumor segmentation approach for MR brain images. *Applied Soft Computing*, 78, 346-354.
24. Shakeel, P. M., Tobely, T. E. E., Al-Feel, H., Manogaran, G., & Baskar, S. (2019). Neural network-based brain tumor detection using wireless infrared imaging sensor. *IEEE Access*, 7, 5577-5588.
25. Ari, A., & Hanbay, D. (2018). Deep learning-based brain tumor classification and detection system. *Turkish Journal of Electrical Engineering & Computer Sciences*, 26(5), 2275-2286.
26. Bahadure, N. B., Ray, A. K., & Thethi, H. P. (2017). Image analysis for MRI based brain tumor detection and feature extraction using biologically inspired BWT and SVM. *International journal of biomedical imaging*, 2017.
27. Corso, J. J., Sharon, E., Dube, S., El-Saden, S., Sinha, U., & Yuille, A. (2008). Efficient multilevel brain tumor segmentation with integrated Bayesian model classification. *IEEE transactions on medical imaging*, 27(5), 629-640.
28. Mallick, P. K., Ryu, S. H., Satapathy, S. K., Mishra, S., Nguyen, G. N., & Tiwari, P. (2019). Brain MRI image classification for cancer detection using deep wavelet autoencoder-based deep neural network. *IEEE Access*, 7, 46278-46287.
29. Li, W., Jia, M., Wang, J., Lu, J., Deng, J. and Tang, J. (2019) Association of MMP9-1562C/T and MMP13-77A/G Polymorphisms with Non-small Cell Lung Cancer in Southern Chinese population. *Biomolecules*, 9(3), 107.
30. Ren, Y. Jiao, X. and Zhang, L. (2018) Expression Level of Fibroblast Growth Factor 5 (FGF5) in the Peripheral Blood of Primary Hypertension Patients and Its Clinical Significance. *Saudi Journal Of Biological Sciences*, 25(3), 469-473.
31. Xiong, Z., Wu, Y., Ye, C., Zhang, X. and Xu, F. (2019) Color image chaos encryption algorithm combining CRC and nine palace map. *Multimedia Tools and Applications*, 78(22), 31035-31055.
32. Yang, L. and Chen, H. (2019) Fault diagnosis of gearbox based on RBF-PF and particle swarm optimization wavelet neural network. *Neural Computing & Applications*, 31(9), 4463-4478.
33. Chen, H., Huang, L., Huang, J., Yang, L., Miao, Y. and Wang, Q. (2020) Model-based method with nonlinear ultrasonic system identification for mechanical structural health assessment. *Transactions on Emerging Telecommunications Technologies*.



ZheShu Jia, female, born on November 1989. 2011-2014, master of computer science of Harbin University of Science and Technology 2015-2019, PHD of School of Computer Science and Technology, Harbin University of Science and Technology. Research field: computer detection and imaging technology, process tomography technology, scientific computing and visualization, artificial intelligence, object-oriented database system.

DEYUN CHEN was born in Harbin on 1962, received doctor degree from Harbin University of Science and Technology in 2006. He is now a full professor and doctoral supervisor in Harbin University of Science and Technology. He has published over 200 scientific papers. His main research interests include detection and imaging technology, image processing and pattern recognition.